

# Morpho-Anatomical and Physiological Analysis of *Cyclocarya paliurus* Provenances for Germplasm Selection in Tea-Style Cultivation

## Çay Tarzı Yetiştiricilikte Germplazm Seçimi İçin *Cyclocarya paliurus* Genotiplerinin Morfo-Anatomik ve Fizyolojik Analizi

Rui CHEN<sup>1</sup>, Seyit YUZUAK<sup>2</sup>, Min WU<sup>3</sup>, Fangping TONG<sup>4</sup>, Sen LIU<sup>5</sup>, Gui LI<sup>6\*</sup>

<sup>1,3,4,5,6</sup> Hunan Academy of Forestry, Department of Forest and Grass Breeding, Changsha, China

<sup>2</sup> Burdur Mehmet Akif Ersoy University, Faculty of Art and Sciences, Department of Molecular Biology and Genetics, Burdur, Türkiye

### Article Info

Research Article

DOI:10.29048/makufebed.1808713

### Corresponding Author

Gui LI

Email: ligui@hnlky.cn

### Article History

Received: 22.10.2025

Revised: 04.12.2025

Accepted: 04.12.2025

Available Online: 29.12.2025

### To Cite

Chen, R., Yuzuak, S., Wu, M., Tong, F., Liu, S., & Gui, L., (2025). Morpho-anatomical and physiological analysis of *Cyclocarya paliurus* provenances for germplasm selection in tea-style cultivation. *The Journal of Graduate School of Natural and Applied Sciences of Mehmet Akif Ersoy University*, 16(2), 117-136. <https://doi.org/10.29048/makufebed.1808713>

**ABSTRACT:** *Cyclocarya paliurus* (Batalin) Iljinsk is an endangered subtropical tree in China with high pharmacological and economic value, yet large-scale cultivation remains limited. Understanding provenance-level variation is critical for identifying elite germplasm suitable for leaf-oriented, tea-style plantations. In this study, seedlings from six natural provenances—Xiushui (XS), Shimen (SM), Lushan (LS), Jianghua (JH), Hupingshan (HP), and Shuangpai (SP)—were grown under tea plantation-style conditions to assess differences in growth, leaf morphology, anatomical structure, physiological traits, stress resistance, and productivity. Clear phenotypic differentiation despite a uniform environment indicates strong genetic control shaped by long-term climatic adaptation processes. Provenances from moderate, mid-elevation climates (SM, SP) showed superior early growth and the highest productivity indices. In contrast, provenances from colder or more thermally variable habitats (LS, XS, HP) exhibited smaller or more compact leaves, higher tissue density, enhanced protective structures, and greater cold or drought resistance. Anatomical features, including mesophyll thickness, stomatal density, and glandular trichome abundance, reflected adaptive trade-offs between carbon assimilation and stress protection. Overall, provenance-specific divergence in leaf form, structure, biomass allocation, and stress-related traits highlights the influence of native climate and supports the targeted selection of high-yield, stress-tolerant germplasm for industrial-scale cultivation.

**Keywords:** *Cyclocarya paliurus*, leaf anatomical traits, provenance variation, stress resistance, tea plantation, germplasm selection

**ÖZ:** *Cyclocarya paliurus* (Batalin) Iljinsk, Çin'de yüksek farmakolojik ve ekonomik değere sahip, ancak büyük ölçekli yetiştiriciliği sınırlı olan nesli tükenme tehlikesindeki bir subtropikal ağaç türüdür. *C. paliurus*'ta menşe düzeyindeki varyasyonların belirlenmesi, yaprak odaklı çay tarzı plantasyon sistemleri için elit genotiplerin seçimi açısından kritik öneme sahiptir. Bu çalışmada, Xiushui (XS), Shimen (SM), Lushan (LS), Jianghua (JH), Hupingshan (HP) ve Shuangpai (SP) menşelerine ait fideler, endüstriyel üretime uygun genotipleri tanımlamak amacıyla çay plantasyonu tarzı koşullar altında yetiştirilmiş ve bir yıllık dönemde büyüme performansı, yaprak morfolojisi, anatomik yapı, fizyolojik özellikler, stres direnci ve verimlilik açısından değerlendirilmiştir. Tekdüze yetiştirme ortamına rağmen belirgin fenotipik farklılıklar gözlenmiş, bu durum güçlü genetik kontrol ve uzun süreli iklim adaptasyonu ortaya koymuştur. ılıman ve orta rakımlı iklim kökenleri (SM, SP) üstün erken büyüme ve daha yüksek verimlilik göstermiştir. Buna karşılık, daha soğuk veya termal açıdan değişken habitat kökenleri (LS, XS, HP) daha kompakt yapraklar, yüksek doku yoğunluğu, gelişmiş koruyucu yapılar ve artmış soğuk veya kuraklık direnci sergilemiştir. Mezofil kalınlığı, stoma yoğunluğu ve salgı tüylerinin bolluğu gibi anatomik özellikler, karbon asimilasyonu ile stres koruması arasındaki uyumsal dengeleri yansıtmıştır. Bu çalışmanın sonuçları, *C. paliurus*'ün farklı menşe özelliklerinin plantasyon koşullarına uyumunda ve yüksek verimli, strese dayanıklı genotiplerin seçiminde önemli bir bilimsel temel sunmaktadır.

**Anahtar Kelimeler:** *Cyclocarya paliurus*, yaprak anatomik özellikleri, genotip varyasyonu, stres direnci, çay plantasyonu, genotip seçimi

## 1. INTRODUCTION

*Cyclocarya paliurus* (Batalin) Iljinsk., belonging to the family Juglandaceae, is a monotypic genus endemic to China, widely distributed in the subtropical regions of southern China (Liu et al., 2022; Liu et al., 2024; Li, 2024). The leaves of *C. paliurus* are rich in various bioactive compounds such as flavonoids, terpenoids, and polysaccharides, which exhibit pharmacological properties such as antioxidant, hypoglycemic, and lipid-lowering effects. These compounds have been primarily developed into functional foods and pharmaceuticals, with large-scale applications in the medicinal tea market (Liu et al., 2018; Zhao et al., 2020; Xu et al., 2023; Wang et al., 2024). However, several intrinsic factors limit the expansion of *C. paliurus* cultivation, such as pronounced seed dormancy and a high rate of seed abortion (Fang et al., 2006; Fang and Wang, 2007; Guo et al., 2024). Moreover, the wild resources are fragmented in distribution, and there are considerable differences in functional traits and bioactive compound contents among different provenances, which significantly constrain its industrial-scale development. Notably, tea plantation-style cultivation combined with dwarfing treatment can increase the leaf yield by more than 30%, offering practical feasibility for large-scale production. Previous studies have demonstrated a strong correlation between leaf anatomical structure and plant yield and stress resistance in tea plants (Wang et al., 2019; Liu et al., 2022; Yang et al., 2024). For instance, the structural variations in *Rhododendron chrysanthum* Pall. leaves contribute to its high level of stress resistance (Guo et al., 2024); similarly, the photosynthetic efficiency and secondary metabolite accumulation in sugarcane are directly influenced by the thickness of palisade tissues and the arrangement of mesophyll cells (Qing et al., 2017). These findings provide a theoretical foundation for the early-stage selection of elite germplasm resources in economic crops based on leaf structure evaluation. As a typical leaf-utilized economic crop, *C. paliurus* exhibits leaf anatomical traits that can serve as important indicators to predict its growth potential (Wang et al., 2023). Anatomical analysis across different provenances growing in the same plantation site reveals that *C. paliurus* leaves commonly possess a single layer of palisade tissue and loosely arranged spongy tissue, with major secondary metabolites distributed in mesophyll cells and glandular trichomes (Zhou et al., 2017). Nevertheless, significant differences exist among provenances in terms of growth traits and secondary metabolite contents (Lan et al., 2022). Therefore, screening based on leaf anatomical structure, combined with cellular-level assessments of photosynthetic efficiency and secondary metabolic potential, can provide a scientific basis for the directional selection of *C. paliurus* cultivars with high yield, superior quality, and strong adaptability under tea-style plantation cultivation systems.

At present, most research on *C. paliurus* has focused on genetic diversity and the contents of functional

components across different provenances. The accumulation patterns of major bioactive compounds are jointly influenced by the genotypes of *C. paliurus* growing in the same plantation site (Sang et al., 2014), and by external environmental factors for natural populations (Sun et al., 2022). However, systematic studies on tea plantation cultivation are still limited, particularly regarding the evaluation of morphological-functional traits, environmental adaptability, and metabolite accumulation patterns among different provenances. This has led to low efficiency in the selection of elite germplasm resources. This study aimed to screen germplasm resources of *C. paliurus* based on leaf characteristics in tea-style plantation cultivation for industrial-scale production.

## 2. MATERIAL and METHODS

### 2.1. Site Description, Sampling, and Measurements

The experimental site is located in Jiaoqiao Village, Longfu Town, Liuyang City, Hunan Province, China (28°25'41.74" N, 113°31'34.73" E). This area is situated in the upper reaches of the Laodao River and belongs to the subtropical monsoon humid climate zone. The annual average temperature in Jiaoqiao Village is 17 °C; the average frost-free period lasts for 264 days per year; the average annual sunshine duration is 1680 h; and the average annual precipitation is approximately 1400 mm.

Leafless branches of *C. paliurus* populations naturally growing in six different provenances outside or at the borders of Hunan, including Xiushui (XS), Shimen (SM), Lushan (LS), Jianghua (JH), Hupingshan (HP), and Shuangpai (SP), were collected, and grafted in the experimental plantation site in Jiaoqiao Village, Liuyang City, Hunan. The linear distances from the provenance sites to the plantation site were 76.01 km (XS), 263.47 km (LS), 262.05 km (HP), 301.77 km (SM), 350.22 km (SP), and 423.72 km (JH) as seen on the map (Figure 1A). Local geographical and climate conditions that characterize the provenance's native habitat were provided in Table 1. The variables include the most extreme temperatures, annual average temperature, annual average humidity, annual rainfall, and altitude range. In March 2024, semi-lignified current-year shoots collected from six different provenances of *C. paliurus* were used as grafting scions. These shoots were grafted onto two-year-old rootstocks obtained from seeds of the same origin and uniform characteristics. The successfully grafted plants were pruned by removing the basal shoots, leaving a single shoot to form the main stem as shown (Figure 1B).

In September 2024, 5 months after grafting, the basal diameter (diameter of the new base at the joint interface between grafted seedling and rootstock) and height of 30 grafted seedlings from six different *C. paliurus* provenances, including XS, SM, LS, JH, HP, and SP, were measured using a digital caliper and tape measure, respectively. For each provenance, the average of three one-year-old seedlings were selected and used for analysis in this study. From each grafted seedling, a total of five

leaves that were healthy, undamaged, mature, and free from harmful insects were sampled from the terminal shoot of the fourth node counted down from the apex (Figure 2A). The collected leaves were immediately sealed

in Ziploc bags and stored in iceboxes for transport back to the laboratory.

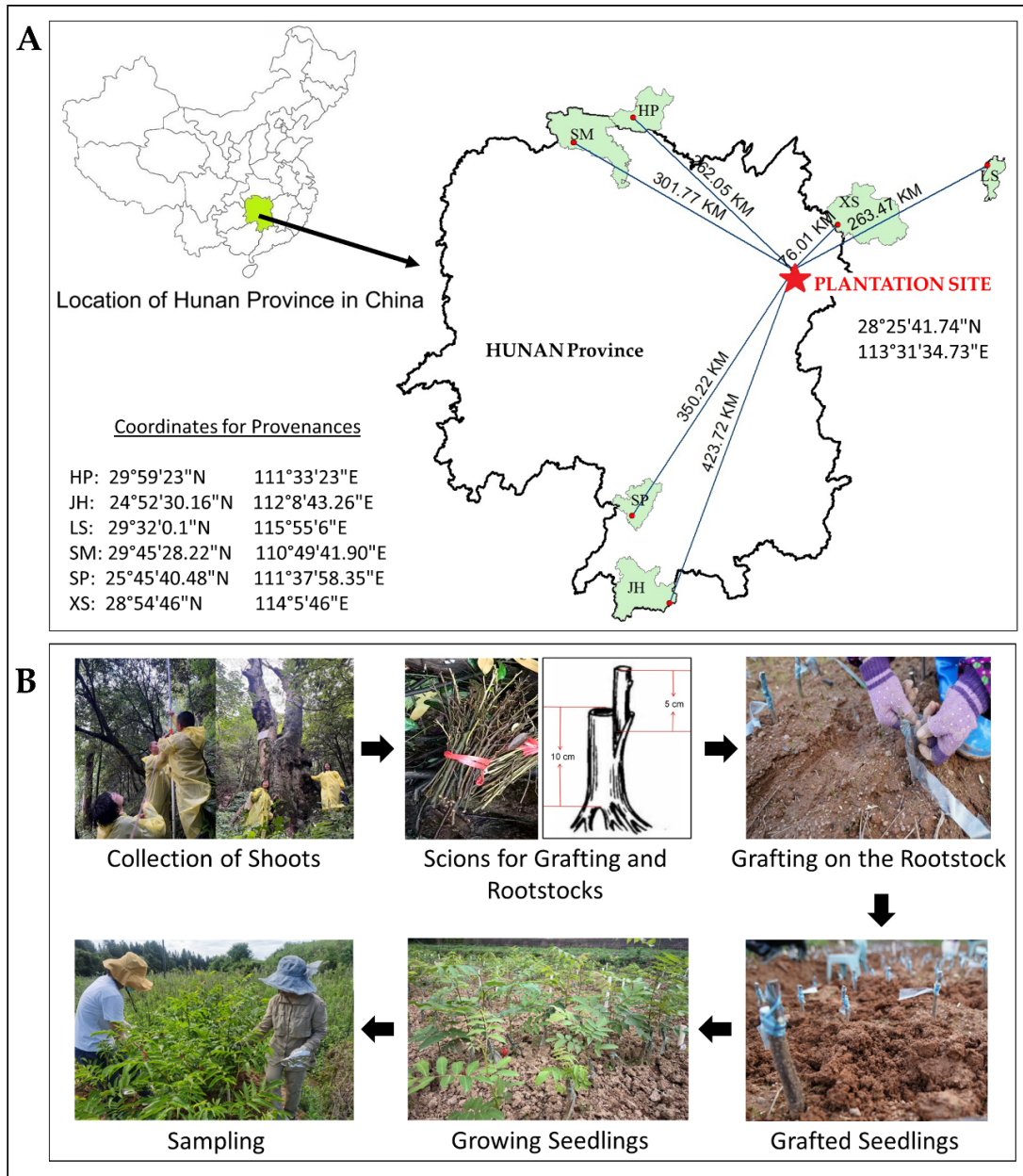


**Figure 1.** Geographical locations of the six provenances of *Cyclocarya paliurus* and the experimental plantation site in Hunan Province, China (A), and pruning, grafting and sampling procedures (B). The left panel of (A) shows the position of Hunan Province within China. Xiushui (XS), Shimen (SM), Lushan (LS), Jianghua (JH), Hupingshan (HP), and Shuangpai (SP).

**Table 1.** Environmental and climate conditions of six different provenances and plantation site

Germplasm ID	The Lowest Temperature so far (°C)	The Highest Temperature so far (°C)	Annual Mean Temperature (°C)	Annual Mean Humidity (%)	Annual Mean Rainfall (mm)	Altitude (m)
HP	-5.7	40.5	16.7	78.0	1286.4	960-1203
JH	-4.8	39.0	18.5	81.0	1510.0	850-900
LS	-10.7	40.2	17.3	75.0	1437.0	450-750
SM	-5	40.9	17.1	75.0	1390.3	450-620
SP	-5.8	40.5	17.7	78.8	1577.2	530-600
XS	-11.6	42.6	16.5	79.0	1575.5	430-755
Plant. Site	-2.5	40.7	17.6	80.0	1562.0	30-180

\*Xiushui (XS), Shimen (SM), Lushan (LS), Jianghua (JH), Hupingshan (HP), and Shuangpai (SP).

To measure the thickness of the leaflets, the first compound leaf at the fourth node from the apex of each grafted seedling was collected. The leaflets on the tip of the selected compound leaf and the single leaflets on each of the second, third, fourth, and fifth leaf pairs were used. Measurements were taken at the upper, middle, and lower spots at a vertical distance of 25 mm from the main vein of each leaflet (Figure 2B), as previously described (Liu et al., 2025). Leaf area (LA), perimeter, and related traits were determined using a DJ-3010P leaf area scanner (Dianjiang Technology Co., Ltd., Shanghai, China). Leaf fresh weight (FW) was measured using a precision electronic balance (0.01 g) (Hochoice, Shanghai, China). Leaves were then soaked in distilled water at 4 °C in the dark for 12 h to obtain saturated fresh weight (SFW), after blotting surface moisture. Subsequently, the leaves were heat-deactivated in an oven at 120 °C for 30 minutes, followed by drying at 80 °C for 24 hours to measure dry weight (DW). Leaf Soil–Plant Analysis Development (SPAD) value, value for the relative amount of total leaf chlorophyll in intact leaves was determined using a portable chlorophyll meter (Zhejiang Top Cloud-Agri Technology Corp., Zhejiang, China). Measurements were taken at three points on both

the main vein and the leaf margin, and the average value was used to represent the chlorophyll content of a single leaf. All measurements were conducted on five leaves per seedling, and mean values were used for subsequent analyses. After measuring leaf area, thickness, and chlorophyll content, average values of the leaf (L.) functional traits were used to calculate specific leaf area (SLA), leaf dry matter content (LDMC), relative water content (RWC), leaf tissue density (LTD), leaf shape index (LSI), and the aspect ratio (AO) for each provenance as follows:

$$SLA = \frac{(\text{Leaf area})}{(\text{Leaf dry mass})} \quad (1)$$

$$LDMC = \frac{(\text{Leaf dry mass})}{(\text{Leaf saturated fresh mass})} \quad (2)$$

$$RWC = \left[ \frac{L. (\text{fresh mass} - \text{dry mass})}{L. (\text{saturated fresh mass} - \text{dry mass})} \right] \times 100 \quad (3)$$

$$LTD = \frac{(\text{Leaf dry mass})}{(\text{Leaf area})} * (\text{Leaf thickness}) \quad (4)$$

$$LSI = \frac{(\text{Leaf area})}{(\text{Leaf length})} * (\text{Leaf width}) \quad (5)$$

$$AO = \frac{(\text{Leaf length})}{(\text{Leaf width})} \quad (6)$$

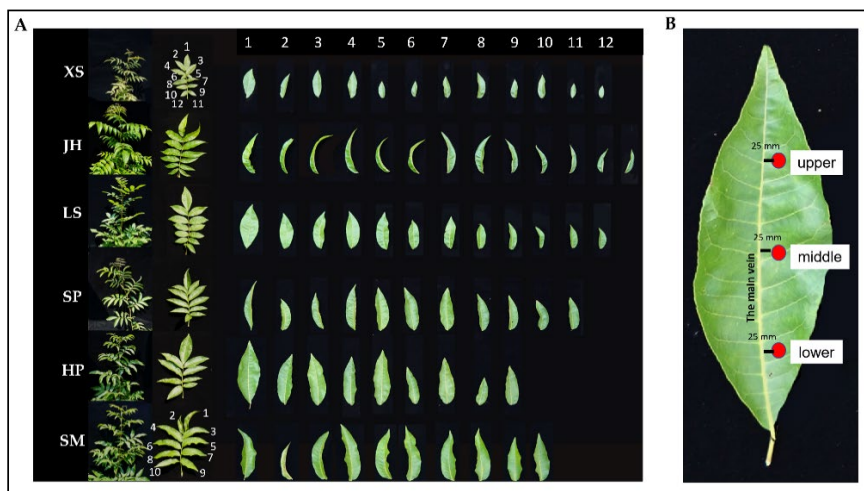


**Figure 2.** Morphological characteristics of *Cyclocarya paliurus* seedlings, compound leaves, and leaflets from six provenances (A) and digital micrometer measurement positions on the unilateral leaflet (B). The columns from left to right in Figure 2A show whole seedlings, compound leaves, and leaflets (1–12) arranged from base to apex, respectively. The third column displays a single branch with attached leaves. All leaflets on the compound leaf were numbered sequentially from the apex (No. 1) to the basal leaflet. XS: Xiushui; JH: Jianghua; LS: Lushan; SP: Shuangpai; HP: Hupingshan; SM: Shimen

## 2.2. Preparation and Observation of Leaf Sections

The fourth fully expanded and healthy leaflet, free from disease, pests, and frost damage, from the top of each *C. paliurus* seedling of different provenances was selected. A tissue block (2 cm × 2 cm) was excised along the main vein and fixed in FAA solution consisting of formalin, glacial acetic acid, and ethanol/DI water (10% formalin / 5% glacial acetic acid / 50% ethanol (95% EtOH) / 35% DI water) for more than 72 h. The samples were submitted to Bio-

Pharmaceutical Accelerator Company (Wuhan, Hubei, China) for microscopic and electron microscopic examination of the relevant microstructure and anatomical analysis. Each sample was photographed three times under an electron microscope at a magnification corresponding to a 200 μm field of view, and the numbers of stomata and glandular trichomes were counted from the 200 μm electron micrographs. The following anatomical traits were measured: upper epidermis thickness (μm, TU), lower epidermis thickness (μm, TL), palisade tissue thickness

( $\mu\text{m}$ , TP), spongy tissue thickness ( $\mu\text{m}$ , TS), leaf thickness (cm, LT), and the number of first-layer palisade cells within a 400  $\mu\text{m}$  range (CA). Subsequently, ratios including palisade tissue thickness to spongy tissue thickness (P/S), palisade tissue thickness to leaf thickness (P/L), upper epidermis thickness to spongy tissue thickness (U/S), spongy tissue thickness to palisade tissue thickness (S/P), spongy tissue thickness to leaf thickness (S/L), productivity index (N), and cold resistance score (Y) were also calculated. Ultimately, 30 groups of data were obtained for each parameter, and the mean values were used for statistical analysis. Productivity index (N) and cold resistance score (Y) were derived using the following formulas:

$$N = CA \times TP \quad (7)$$

$$\text{Cold Resistance Score} = \left[ 5.47 \times \frac{TP}{TS} \right] - 1.78 \quad (8)$$

Each parameter was measured using 15 biological replicates, and the mean values were used for statistical analysis.

### 2.3. Data Processing

Basic statistical analyses of leaf morphological and anatomical trait data were performed using WPS Office Software (Kingsoft Corp., Beijing, China). The coefficient of variation (CV) is defined as the ratio of the standard deviation to the mean, expressed as a percentage (%). The Shannon-Weaver genetic diversity index ( $H'$ ) is defined as gene diversity or expected heterozygosity. The CV was calculated for each parameter. Because the Shannon-Weaver information index is defined for discrete variables, each quantitative leaf morphological and anatomical trait was first discretized prior to calculation. For each trait, the continuous values were divided into [X] classes; 1–10) using an equal-interval binning method (or quantile-based binning). The relative frequency ( $P_i$ ) of individuals within each class is then calculated, and the Shannon-Weaver index is computed using the following formula (Wang et al., 2019);

$$H' = - \sum P_i \ln P_i \quad (9)$$

Where  $P_i$  is the frequency of occurrence of the  $i$  code of a trait. Before calculating the genetic diversity index ( $H'$ ), the quantitative traits of six different provenances were subjected to qualitative treatment, and the numerical traits were classified into 10 levels based on the mean as the center, with half the standard deviation as the step size: level 1  $< \bar{X} - 2s$ , level 10  $\geq \bar{X} + 2s$  each level difference in the middle 0.5s,  $\bar{X}$  is the mean and  $s$  is the standard deviation. A statistically reasonable category interval of 0.5s was used to support the calculation of the Shannon index, to prevent instability in probability estimates due to categories with small sample sizes, and to ensure that samples are distributed sufficiently and equally across categories. This made the  $H'$  value more robust and

reliable. The Shannon-Weaver information index was used to calculate the diversity of leaf morphological and anatomical traits.

Stress resistance evaluation was conducted using the fuzzy mathematics membership function method. The calculation formula is:

$$f(x_i) = (x_i - x_{\min}) / (x_{\max} - x_{\min}) \quad (10)$$

Where  $i = 1, 2, 3, 4, 5, 6$ , and  $x_i$  represents the measured value of a given trait, and  $x_{\max}$  and  $x_{\min}$  represent the maximum and minimum values of that trait among all *C. paliurus* leaf anatomical characteristics, respectively.

In this study, all grafted seedlings were grown in the same plantation site. Throughout their growth, the plants were not directly exposed to any biotic or abiotic stress conditions. Therefore, all resistance indices were obtained indirectly based on data derived from calculated leaf parameters, measurements, and formulas used. A comprehensive evaluation of stress resistance was obtained by calculating the mean membership function value (MM) of each relevant trait, with a higher MM value indicating stronger resistance to stress (Wang et al., 2019). Multivariate statistical analyses were performed using IBM SPSS 20.0 software (IBM Corp., Armonk, NY, USA). Principal component analyses (PCA) were conducted using the criterion of eigenvalues  $> 1.0$ , and dimensionality reduction was achieved via principal component extraction. A distance matrix was constructed, and principal coordinate analysis (PCoA) was performed to reveal differences in overall environmental and climatic conditions among the provenances and the plantation site, and in leaf anatomical characteristics among seedlings of each provenance grown at the plantation site. It is implemented through an indirect method of distance matrix calculation and factor analysis (as an alternative for dimensionality reduction). The core idea is to first calculate the inter-sample distance matrix based on climatic data, then perform dimensionality reduction and visualization on the distance matrix, and finally achieve the classification of provenances and plantation sites. Hierarchical cluster analysis was performed using Ward's minimum variance method, with squared Euclidean distance employed to measure genetic distance among germplasm. After analysis of variance (ANOVA), the least significant difference (LSD) test was used for multiple comparisons of anatomical traits among different clusters.

## 3. RESULTS

### 3.1. Key Climate Factors in Six Different Provenances and Plantation Site

Key climate factors in six different provenances of *C. paliurus* (Xiushui (XS), Shimen (SM), Lushan (LS), Jianghua (JH), Hupingshan (HP), and Shuangpai (SP)) along with the plantation site as presented in Table 1 were assessed. For temperature regimes, minimum temperatures ranged

from  $-11.6^{\circ}\text{C}$  (XS) to  $-4.8^{\circ}\text{C}$  (JH), indicating substantial variation in winter severity across provenances. Provenances LS and XS experience the coldest minimums, whereas JH and HP inhabit comparatively milder winter environments. Maximum historical temperatures span from  $39.0^{\circ}\text{C}$  (JH) to  $42.6^{\circ}\text{C}$  (XS), suggesting that XS is exposed to both the lowest and highest temperature extremes. Annual mean temperatures vary moderately among sites ( $16.5\text{--}18.5^{\circ}\text{C}$ ), with JH exhibiting the warmest average conditions and HP the coolest. For humidity and rainfall, annual average humidity ranges between 75% and 81%. JH shows the highest humidity (81%), whereas LS and SM have the lowest (75%), indicating slightly drier atmospheric conditions in the latter. Rainfall levels are uniformly high across provenances (1286–1577 mm), consistent with humid subtropical climates. SP and XS receive the highest annual precipitation ( $>1570$  mm), while HP receives the least (1286 mm), suggesting variation in hydrological availability that may influence physiological adaptation. For altitude, provenances span a wide range of elevation conditions. HP is located at the highest altitudes (960–1203 m), while LS, SM, SP, and XS occupy mid-elevation habitats (approximately 430–755 m). The plantation site lies at a substantially lower elevation (30–180 m), representing a markedly different ecological context from all natural provenances.

### 3.2. Growth Performance of *C. paliurus* Provenances

Seedling growth traits varied significantly across the six provenances of *C. paliurus* (Table 2). Lushan (LS) exhibited the greatest vigor, with the highest seedling height ( $0.87 \pm 0.05$  m) and basal stem diameter ( $1.03 \pm 0.05$  cm). Shimen (SM) ranked second, with growth metrics statistically comparable to LS yet significantly exceeding those of the remaining provenances. In contrast, Jianghua (JH) displayed the weakest growth performance, suggesting limited adaptability under the environmental conditions of the plantation site.

**Table 2.** Growth performance of *Cyclocarya paliurus* seedlings from six provenances

Seed source	Seedling height (m)	Basal diameter (cm)
HP	$0.60 \pm 0.05\text{c}$	$0.66 \pm 0.05\text{c}$
JH	$0.57 \pm 0.03\text{d}$	$0.59 \pm 0.04\text{d}$
LS	$0.87 \pm 0.05\text{a}$	$1.03 \pm 0.05\text{a}$
SM	$0.79 \pm 0.05\text{ab}$	$0.97 \pm 0.06\text{ab}$
SP	$0.68 \pm 0.05\text{bc}$	$0.81 \pm 0.04\text{bc}$
XS	$0.62 \pm 0.05\text{c}$	$0.70 \pm 0.04\text{c}$

\* Data represent mean  $\pm$  SE for grafted seedling height (m) and basal diameter (cm) of current-year-old grafted seedlings. Different lowercase letters among different provenances indicate significant differences in seedling height and caliper diameter ( $p \leq 0.05$ , LSD test). XS: Xiushui, SM: Shimen, LS: Lushan, JH: Jianghua, HP: Hupingshan, and SP: Shuangpai.

Based on the key environmental and climatic factors (minimum and maximum historical temperature, humidity, rainfall, altitude) from the six *C. paliurus* provenances and the plantation site, a distance matrix was constructed, and principal coordinate analysis (PCoA) was performed (Figure 3; Supplementary Table 1). The climatic distance matrix histogram (Figure 3A) revealed substantial variability among the six *C. paliurus* provenances and the plantation site (PS). Distances ranged from 2.4 to 5.5, with the smallest climatic difference observed between SP–PS, and the largest between HP–PS. The histogram demonstrates a right-skewed distribution, suggesting that several provenance pairs have relatively large climatic dissimilarities. This reflects a broad environmental gradient

across the provenances and plantation site, incorporating variation in temperature extremes, annual means, humidity, rainfall, and elevation. The first two PCoA axes explained 59.94% of the total variation (PCoA1 = 33.64%, PCoA2 = 26.30%). The ordination clearly separates the provenances and plantation sites (Figure 3b) along major climatic gradients: XS is positioned distinctly on the upper right of PCoA space, indicating unique climatic characteristics and the greatest divergence from other sites. HP and JH cluster separately at the lower left and lower center region, respectively, indicating climatic environments different from LS, SM, SP. LS and SM are located near each other, implying high climatic similarity. SP occupies an intermediate position, consistent with moderate distances in the matrix. PS is separated along PCoA1, reflecting substantial divergence from the other provenances.

Leaf trait variation at the plantation site was strongly associated with the climatic divergence among provenances. Provenances originating from cooler and more seasonal environments (HP, JH) expressed more conservative leaf traits, including smaller leaf area, thicker leaves, and lower stomatal density, consistent with adaptations to low-temperature stress and hydraulic limitation. In contrast, provenances from warm and humid regions (LS, SM, SP, XS) expressed more acquisitive traits at the plantation site, such as larger leaves, higher chlorophyll content, and greater stomatal densities, reflecting their adaptation to high-resource environments. Notably, XS—identified as the most climatically distinct provenance in the PCoA—also showed the most divergent leaf trait expressions, highlighting the strong influence of origin climate. Overall, climatic distance among provenances was mirrored by their leaf functional differentiation under common plantation site conditions, suggesting that local climatic adaptation is a major driver of intraspecific trait variation in *C. paliurus*. The PCoA and heatmap analyses consistently demonstrate a strong climatic divergence among *C. paliurus* provenances

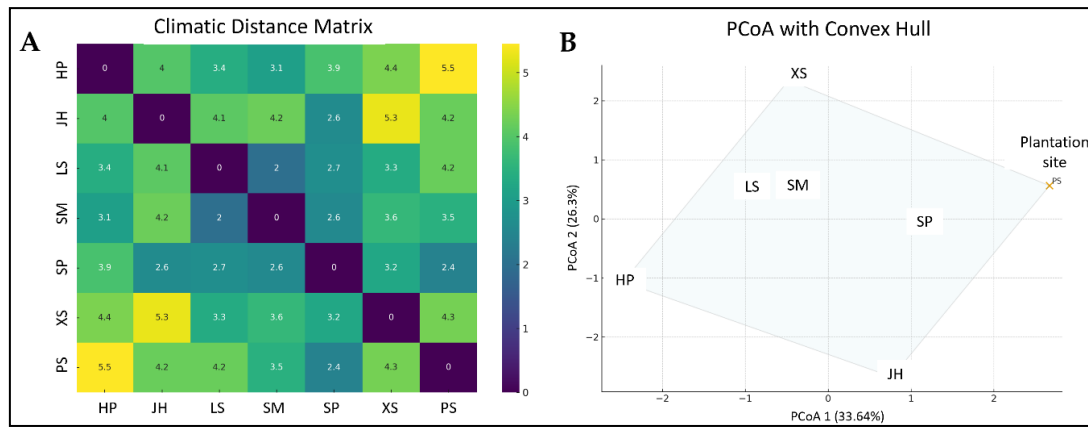


**Figure 3.** Climatic distance matrix (A) and principal coordinate analysis (PCoA) (B) based on the key environmental and climatic factors from the six *Cyclocarya paliurus* provenances and the plantation site. The convex hull illustrates the climatic "envelope" encompassing all sites, emphasizing the wide environmental heterogeneity spanned by the provenances and the plantation site. XS: Xiushui; JH: Jianghua; LS: Lushan; SP: Shuangpai; HP: Hupingshan; SM: Shimen; PS: plantation site

### 3.3. Comparison of Leaf Anatomy and Morphology Across Provenances

The leaf anatomy and morphology trait analysis revealed significant differences ( $P < 0.01$ ) in leaf area, vertical length, aspect ratio, shape index, fresh weight, and saturated fresh weight among *C. paliurus* provenances (Figure 4). Specific leaf area (Eq. 1) ranged from 11.32 to 47.27 cm<sup>2</sup> (mean 32.17 cm<sup>2</sup>), ranking HP > SM > LS > JH > SP > XS. HP produced leaves 4.18 times larger than XS, with extremely significant differences between XS and all other provenances, and between HP and LS, JH, and SP. Leaf perimeter (mean 26.46 cm) followed a similar pattern, as HP values nearly doubled those of XS ( $P < 0.01$ ). Vertical length (mean 4.03 cm) showed the same order, with HP almost twice XS. Horizontal width (mean 10.73 cm) ranked SM > HP > SP > JH > LS > XS, with SM 91% greater than XS. XS consistently produced the smallest leaves, reflecting a compact morphology. SP exhibited the highest aspect ratio (3.27) (Eq. 6), while HP recorded the highest leaf shape index (0.61) (Eq. 5). Overall, HP displayed broad morphological variability, whereas SP formed narrower leaves, indicating distinct adaptive strategies. Significant differences observed in leaf morphology and anatomical structure among *C. paliurus* provenances indicated clear differentiation in morphological and anatomical adaptations to diverse environmental conditions.

The substantial morphological and anatomical differentiation observed among *C. paliurus* provenances is closely aligned with the ecological and climatic heterogeneity characterizing their regions of origin. Provenances such as HP, native to higher-altitude and cooler environments, produced the largest leaves—exhibiting the greatest leaf area, perimeter, vertical length, and shape index. In contrast, XS, which originates from regions with greater thermal extremes and colder historical minima, produced the smallest and most compact leaves. These results demonstrate that leaf morphology and anatomical structure in *C. paliurus* are strongly influenced by provenance-specific environmental

conditions, including temperature regimes, precipitation, humidity, and altitude. The clear morphological divergence among provenances under a uniform plantation environment highlights the role of local adaptation in shaping leaf functional traits. These inherent differences also underscore the importance of considering climatic origin when selecting germplasm for tea-style plantation cultivation, given that leaf size, shape, and anatomical characteristics directly impact leaf biomass yield and potential industrial value.

### 3.4. Differences in Leaf Biomass Among Provenances of *C. paliurus*

Leaf biomass differed significantly among provenances. Figure 4 shows that leaf thickness (LT) in *C. paliurus* ranged from 0.153 to 0.188 cm (mean 0.17 cm). LS produced the thickest leaves, 23% greater than SP and SM, suggesting enhanced capacity for photosynthetic tissue and biomass accumulation. Chlorophyll content ranged from 26.15 to 36.36, with JH reaching the highest level, 39% above XS, indicating greater potential for light energy conversion. HP recorded the highest biomass traits, including fresh weight (0.71 g), saturated fresh weight (0.82 g), and dry weight (0.23 g), with fresh weight exceeding XS by more than fivefold. By contrast, XS produced the lowest biomass but maintained the highest relative water content (85.34%) (Eq. 3), tissue density (0.04 g·cm<sup>-3</sup>) (Eq. 4), and dry matter content (0.42 g·g<sup>-1</sup>) (Eq. 2). SM exhibited the highest specific leaf area (287.47), consistent with a rapid growth strategy under high-light conditions.

The differences in leaf biomass among *C. paliurus* provenances can be largely interpreted through the ecological and climatic characteristics of their native habitats. Provenances originating from cooler, higher-altitude, or more variable thermal environments exhibit leaf structural and physiological traits distinct from those native to relatively moderate or stable climates, reflecting long-term local adaptation. Provenances such as HP, which produced the highest leaf biomass (fresh, saturated, and

dry weight), originate from high-altitude regions with relatively low annual temperatures. In contrast, XS displayed the lowest leaf biomass, yet possessed the highest relative water content, tissue density, and dry matter content. XS originates from regions with harsher

winter temperature minima (-11.6°C), and its biomass pattern reflects a conservative resource-use strategy commonly associated with stress-prone environments.

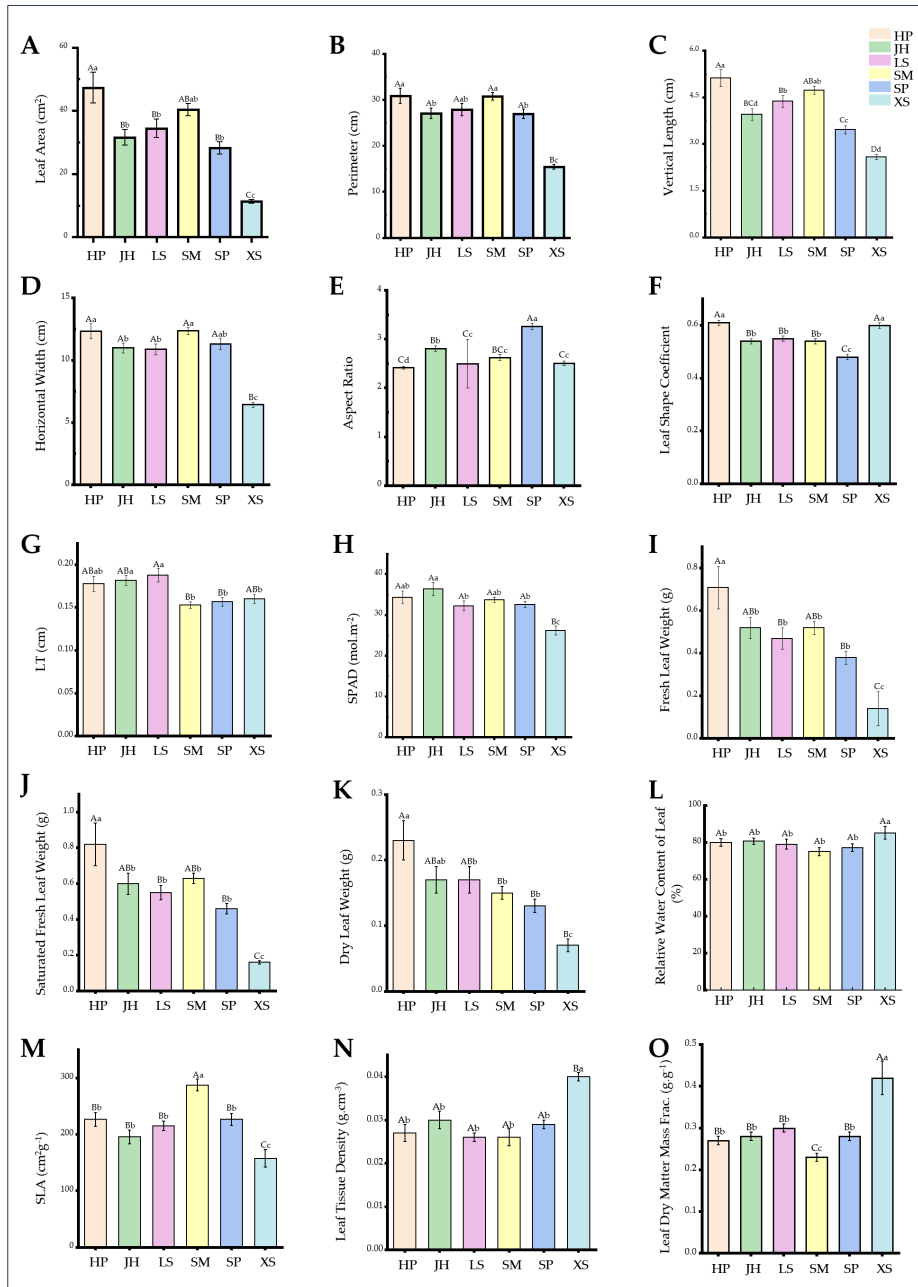


**Figure 4.** Variation in morphological and physiological leaf traits among *Cyclocarya paliurus* provenances. Traits measured include leaf area (A), perimeter (B), vertical length (C), horizontal width (D), aspect ratio (E), leaf shape coefficient (F), leaf thickness (G), SPAD value (H), specific leaf weight (I), saturated fresh leaf weight (J), dry leaf weight (K), relative water content of the leaf (L), tissue mass per area (M), stomatal density (N), and leaf dry matter content (O). Bars represent means ± SE. In the bar charts of leaf morphological and physiological traits of different provenances, bars with different uppercase letters indicate extremely significant differences ( $p \leq 0.01$ , LSD test), and bars with different lowercase letters indicate significant differences ( $p \leq 0.05$ , LSD test). LS: Lushan; XS: Xiushui; SM: Shimen; JH: Jianghua; HP: Hupingshan; SP: Shuangpai

### 3.5. Provenance-Level Genetic Variation in Leaf Structural Traits

Analysis of 27 structural leaf parameters across six *C. paliurus* provenances (Figure 5; Tables 3 and 4) revealed

significant morphological and anatomical differences, demonstrating rich genetic variation at the provenance level. Genetic diversity indices (Eq. 9) were highest for the palisade-to-spongy tissue ratio ( $H' = 1.92$ ), followed by leaf dry matter content, leaf shape index, leaf tissue density,

and the ratio of upper epidermis to spongy tissue thickness (all  $H' \approx 1.90$ ). These values indicate substantial genetic resources for targeted selection and breeding in germplasm improvement. Coefficients of variation (CV) further highlighted trait-specific differences: leaf fresh weight showed the highest variation (14.67%), reflecting sensitivity to environmental factors and indicating genetic differences among provenances, whereas leaf shape index showed the lowest (1.83%), suggesting relative stability across provenances.

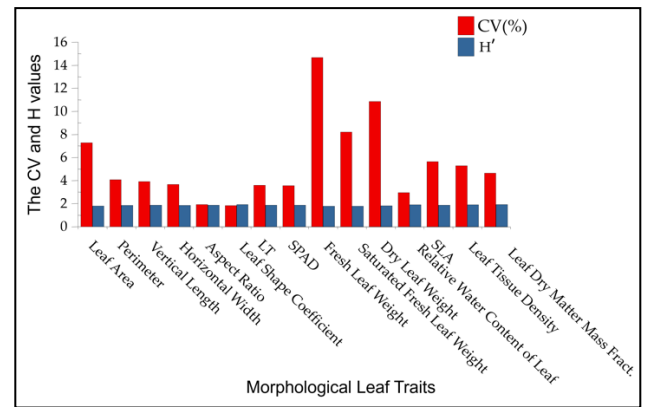


**Figure 5.** Coefficient of variation (CV, red bars) and Shannon diversity index ( $H'$ , blue bars) for leaf morphological, anatomical, and physiological traits across six provenances of *Cyclocarya paliurus*.

**Table 3.** Anatomical traits of leaves and petioles of *Cyclocarya paliurus* from six provenances

Germplasm ID	TU ( $\mu\text{m}$ )	TP ( $\mu\text{m}$ )	TS ( $\mu\text{m}$ )	TL ( $\mu\text{m}$ )	Petiole Thickness ( $\mu\text{m}$ )	Stomatal Number on the Lower Epidermis
HP	12.01±0.36ABb	45.38±7.12A	57.60±5.30ABb	11.82±1.43ABb	781.1±33.16Aa	83.00±19.01Aa
JH	14.47±1.09Aa	55.02±4.05A	76.59±6.36Aa	14.49±0.20Aa	688.93±34.02Ab	96.33±2.68Aa
LS	10.07±0.47Bc	43.44±0.86A	42.56±1.69Bc	10.11±0.24Bb	759.90±37.53Aa	108.00±2.08Aa
SM	10.63±0.26Bb	49.23±5.80A	48.65±6.83Bbc	10.73±0.70Bb	790.50±6.81Aa	110.00±14.47Aa
SP	12.28±0.96ABb	53.64±2.25A	63.86±1.57ABab	11.85±1.00ABb	737.07±24.67Aa	103.00±13.45Aa
XS	10.45±0.26Bb	54.69±0.44A	41.86±1.18Bc	9.38±0.21Bc	508.27±10.56Bc	88.00±2.52Aa
GR	11.65	50.23	55.19	11.40	710.96	98.00
CV%	4.66	6.97	6.80	5.51	3.40	9.45
H	1.84	1.87	1.80	1.83	1.86	1.85

\* GR: grand mean; CV: coefficient of variation; H: Shannon diversity index. Values are means  $\pm$  SE. Different uppercase letters indicate extremely significant differences ( $p \leq 0.01$ , LSD test) in the anatomical traits of the leaves and petioles among different provenances, while different lowercase letters indicate significant differences ( $p \leq 0.05$ , LSD test) in the anatomical traits of the leaves and petioles among the different provenances. TU: upper epidermis thickness; TP: palisade tissue thickness; TS: spongy tissue thickness; TL: lower epidermis thickness. XS: Xiushui; SM: Shimen; LS: Lushan; JH: Jianghua; HP: Hupingshan; SP: Shuangpai.

**Table 4.** Anatomical traits of *Cyclocarya paliurus* leaves from six provenances

Germplasm ID	P/S	P/L	U/S	S/P	S/L	N
HP	0.79±0.13Bc	0.27±0.07Aa	0.21±0.02Aab	1.32±0.19ABa	0.33±0.03Aa	2014.10±289.53Aa
JH	0.72±0.01Bc	0.30±0.05Aa	0.19±0.01Ab	1.39±0.02Aa	0.41±0.07Aa	2269.09±208.70Aa
LS	1.02±0.05ABbc	0.24±0.02Aa	0.24±0.02Aab	0.98±0.05Bb	0.24±0.03Ab	1664.72±41.63Bb
SM	1.03±0.10ABb	0.32±0.07Aa	0.23±0.03Aab	0.99±0.09Bb	0.31±0.08Aa	2506.97±144.93Aa
SP	0.84±0.04Bbc	0.34±0.03Aa	0.19±0.01Ab	1.19±0.05ABab	0.40±0.04Aa	2334.12±78.79Aa
XS	1.31±0.03Aa	0.35±0.01Aa	0.25±0.01Aa	0.76±0.01Bb	0.27±0.01Aa	2296.52±91.98Aa
GR	0.95	0.30	0.22	1.11	0.33	2180.92
CV%	6.62	14.33	7.71	5.92	12.97	6.54
H'	1.92	1.87	1.91	1.83	1.81	1.87

\* GR: grand mean; CV: coefficient of variation; H': Shannon diversity index. Values are means  $\pm$  SE. Different uppercase letters indicate extremely significant differences ( $p \leq 0.01$ , LSD test) in the anatomical traits of the leaves and petioles among different provenances, while different lowercase letters indicate significant differences ( $p \leq 0.05$ , LSD test) in the anatomical traits of the leaves and petioles among different provenances. Ratios including P/S: palisade tissue thickness to spongy tissue thickness; P/L: palisade tissue thickness to leaf thickness; U/S: upper epidermis thickness to spongy tissue thickness; S/P: spongy tissue thickness to palisade tissue thickness; S/L: spongy tissue thickness to leaf thickness; N: productivity index. XS: Xiushui; SM: Shimen; LS: Lushan; JH: Jianghua; HP: Hupingshan; SP: Shuangpai.

### 3.6. Anatomical Differences of Leaves among *C. paliurus* Provenances

Microscopic analyses revealed typical dorsiventral anatomy, with single-layered epidermal cells, palisade tissues of elongated columnar cells, and loosely arranged spongy tissues (Figures 7 and 8). Significant inter-provenance differences (Tables 3 and 4) were observed in epidermal and mesophyll tissues. JH displayed the thickest upper (14.47  $\mu\text{m}$ ) and lower epidermis (14.49  $\mu\text{m}$ ), whereas XS recorded the lowest values. Spongy tissue thickness was greatest in JH (76.59  $\mu\text{m}$ ) and SP (63.86  $\mu\text{m}$ ), while XS showed the lowest value (41.86  $\mu\text{m}$ ). Ratios of palisade-to-spongy tissue (P/S) and spongy-to-leaf thickness (S/L) also differed significantly, reflecting contrasting photosynthetic and water-use strategies. Petiole thickness was greatest in SM (790.50  $\mu\text{m}$ ), suggesting enhanced vascular transport, while XS had the lowest value. SEM images (Figures 9 and 10) revealed thick cuticles, wavy epidermal walls, and trichomes on both surfaces, denser on the lower epidermis. Stomata appeared only on the lower epidermis. Stomatal density followed the order SM > LS > SP > JH > XS > HP, whereas glandular trichome density exhibited the opposite trend (Figure 11). This inverse relationship suggests a potential trade-off between gas exchange and protective functions.

A principal coordinate analysis (PCoA) based on combined environmental variables and leaf anatomical characteristics revealed that leaf anatomical traits of *C. paliurus* exhibit clear provenance-specific structuring that is tightly linked to climatic origin, indicating adaptive differentiation among provenances (Figure 6). The first axis (PCoA1) captured the major gradient associated with rainfall, temperature extremes, and anatomical thickness traits (TP, TS, TL, petiole thickness). The second axis (PCoA2) described variation related mostly to humidity, epidermal thickness (TU, TL), and altitude. PCoA1 values were -4.270 (XS), -1.597 (LS), -0.351 (SM), 0.200 (SP), 2.941 (JH), and 3.078 (HP), while PCoA2 values are -1.257 (XS), 2.914 (LS), 1.666 (SM), -1.611 (SP), -3.576 (JH), and 1.863 (HP). Provenances such as HP and JH clustered at the positive end of PCoA1, characterized by warmer climates, higher precipitation, and greater tissue thickness. In contrast, XS and LS, originating from cooler areas with lower rainfall, grouped toward the negative end and exhibited thinner palisade and spongy tissues. Provenances LS, SM, and HP scored higher on PCoA2, indicating association with higher humidity and thicker epidermal layers. JH, SP, and XS occupied the opposite end, reflecting comparatively lower epidermal development and environmental moisture.

Differences in epidermal thickness, mesophyll structure, stomatal distribution, and protective features such as cuticle development and trichome density appear to be closely related to the temperature, humidity, precipitation, and altitudinal gradients from which these provenances originate. Provenances such as JH, which demonstrated the thickest upper and lower epidermis and the most

developed spongy tissues, originate from warm, humid environments with consistently high annual temperatures and humidity. Such conditions typically favour anatomical traits that enhance gas exchange efficiency and support robust photosynthetic activity, including thicker epidermal layers for maintaining leaf turgor under humid conditions and expanded spongy tissues facilitating internal CO<sub>2</sub> diffusion. The high palisade- and spongy-tissue development in JH therefore aligns with a strategy optimized for light capture and high photosynthetic capacity in moisture-rich habitats. In contrast, XS—which originates from regions with the lowest historical minimum temperatures and substantial thermal variability—consistently exhibited the smallest values for epidermal thickness, mesophyll development, and spongy-tissue thickness. These traits align with cold-adaptive strategies that minimize metabolic expenditure, reduce surface area for heat loss, and maintain structural efficiency in environments where low temperatures constrain photosynthetic rates. Similarly, petiole thickness—greatest in SM and smallest in XS—reflects differences in hydraulic transport capacity that correspond to provenance-specific water availability and growth strategies. Provenances from regions with higher rainfall and humidity (SM, JH) may evolve greater vascular conductance to support high photosynthetic rates, whereas those from colder or more variable climates (XS) adopt conservative hydraulic strategies.

Stomatal density and glandular trichome density also showed clear ecological patterns. Provenances such as SM and LS, which are native to mid-elevation habitats with higher solar radiation and greater evaporative demand, exhibited higher stomatal density, supporting enhanced carbon assimilation under high-light conditions. Conversely, provenances such as HP and XS displayed higher glandular trichome density, consistent with an increased need for improved protection against cold, UV stress, or water loss.

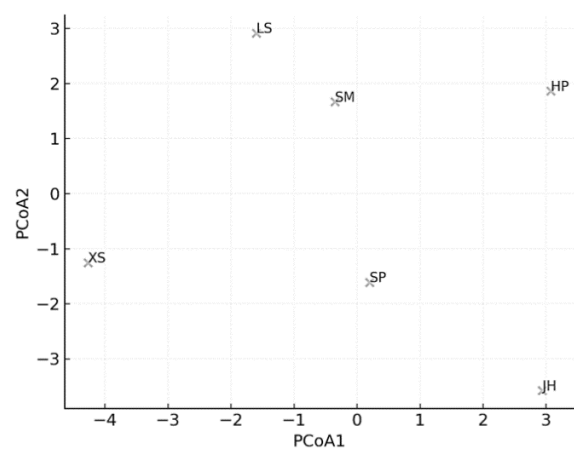


**Figure 6.** Two-dimensional Principal Coordinates Analysis (PCoA) performed to group the six different provenances based on climatic differences and leaf anatomical characteristics observed at the plantation site. XS: Xiushui; SM: Shimen; LS: Lushan; JH: Jianghua; HP: Hupingshan; SP: Shuangpai.

Collectively, these anatomical disparities among *C. paliurus* provenances demonstrate the strong influence of native climatic factors—including temperature extremes, precipitation regimes, humidity levels, and elevation—on the evolution of leaf structural traits. When grown under a common plantation environment, these inherent anatomical differences persist, highlighting their adaptive value and underscoring the importance of considering climatic origin in germplasm selection for leaf-based industrial cultivation.

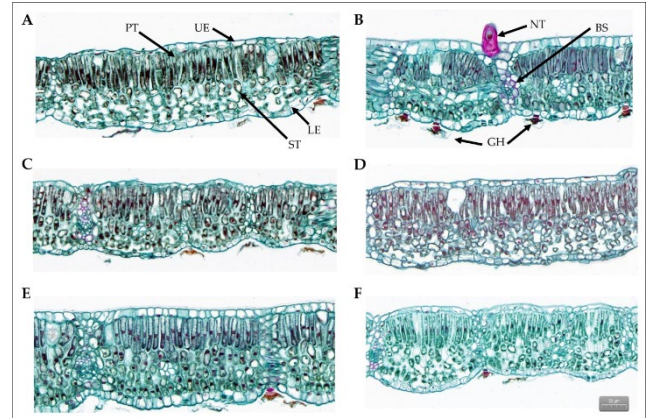


**Figure 7.** Transverse sections of leaves from six *Cyclocarya paliurus* provenances (A–F). A: Hupingshan; B: Jianghua; C: Lushan; D: Shimen; E: Shuangpai; F: Xiushui provenances. PT: palisade tissue; UE: upper epidermis; ST: spongy tissue; LE: lower epidermis; NT: non-glandular trichome; BS: bundle sheath; GH: glandular hair. Scale bar: 50  $\mu\text{m}$ .

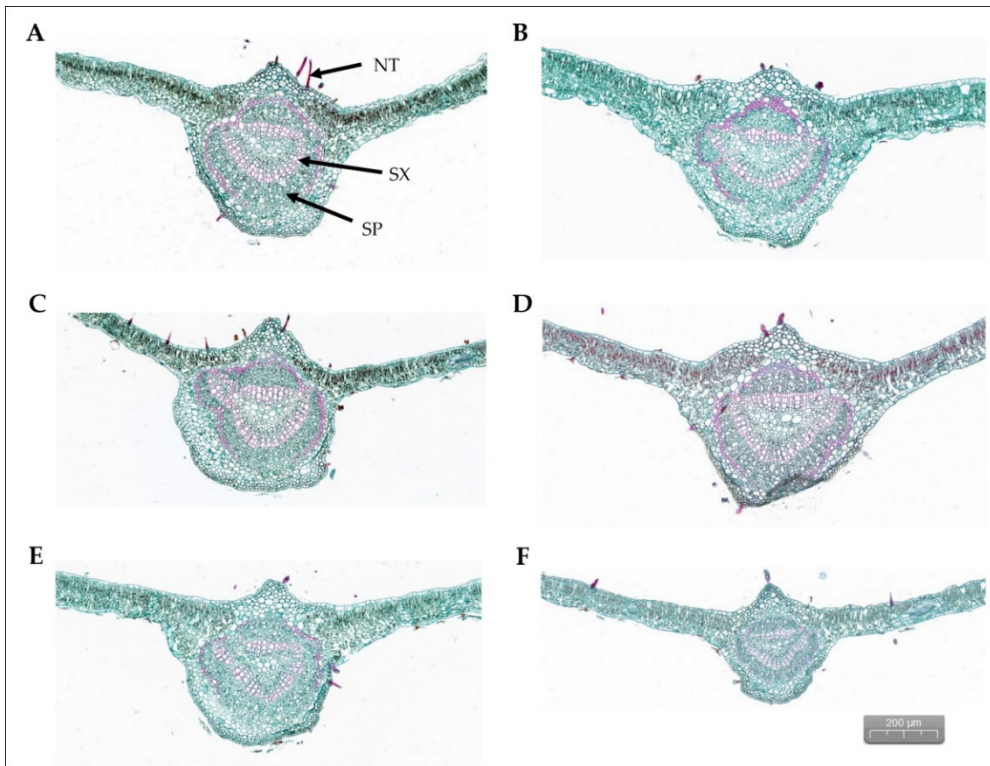


**Figure 8.** Transverse sections of midribs from six *Cyclocarya paliurus* provenances (A–F). A: Hupingshan; B: Jianghua; C: Lushan; D: Shimen; E: Shuangpai; F: Xiushui provenances. NT: non-glandular trichome; SX: secondary xylem; SP: secondary phloem. Scale bar: 200  $\mu\text{m}$ .

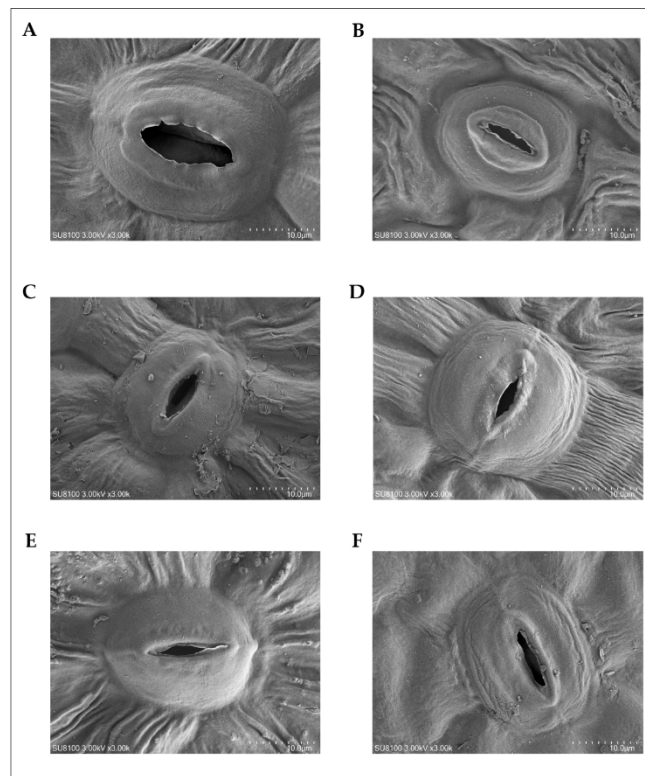


**Figure 9.** Scanning electron micrographs of stomata on the abaxial leaf epidermis of *Cyclocarya paliurus* from six provenances (A–F). Stomatal shape, aperture size, and guard cell morphology vary among provenances. Images were taken at 3,000× magnification. Scale bar = 10 µm. A: Hupingshan; B: Jianghua; C: Lushan; D: Shimen; E: Shuangpai; F: Xiushui.

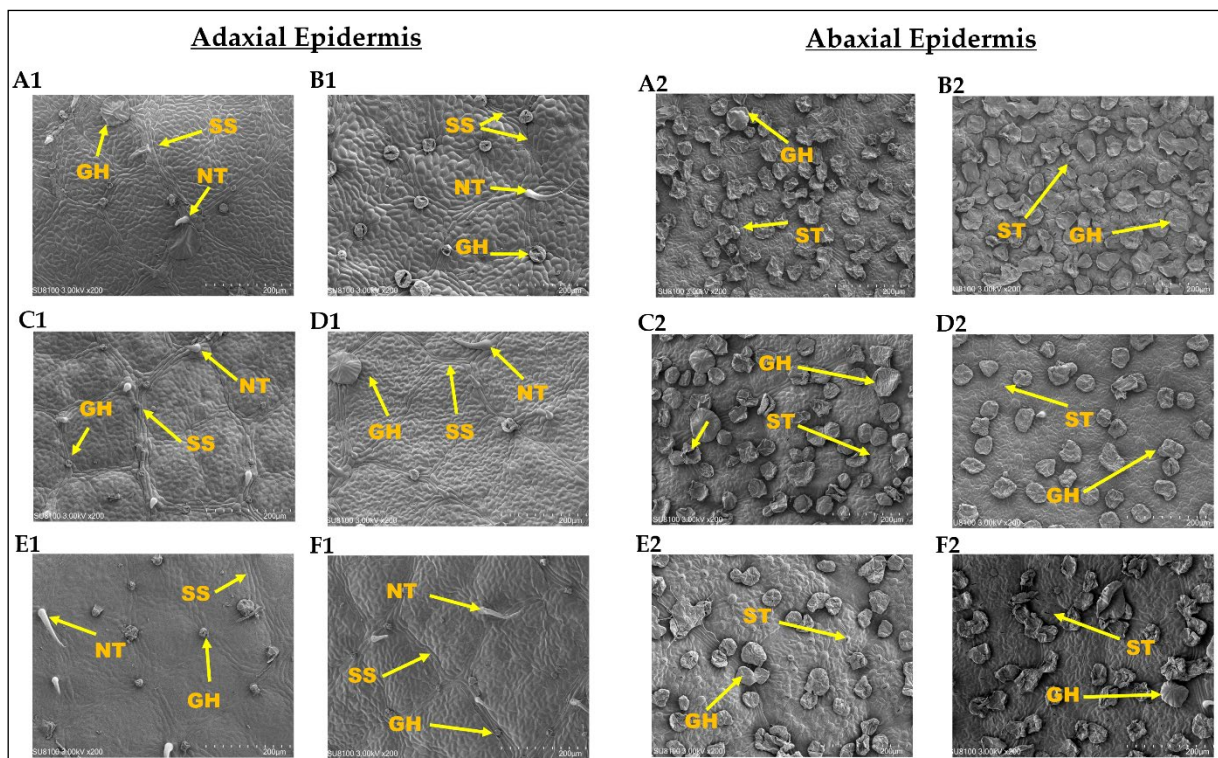


**Figure 10.** Scanning electron micrograph of adaxial (A1–F1) and abaxial (A2–F2) leaf epidermis of six *Cyclocarya paliurus* provenances. SS: stomatal structure; NT: non-glandular trichome; GH: glandular hair; ST: stomata. Scale bars = 200 µm. A: Hupingshan; B: Jianghua; C: Lushan; D: Shimen; E: Shuangpai; F: Xiushui

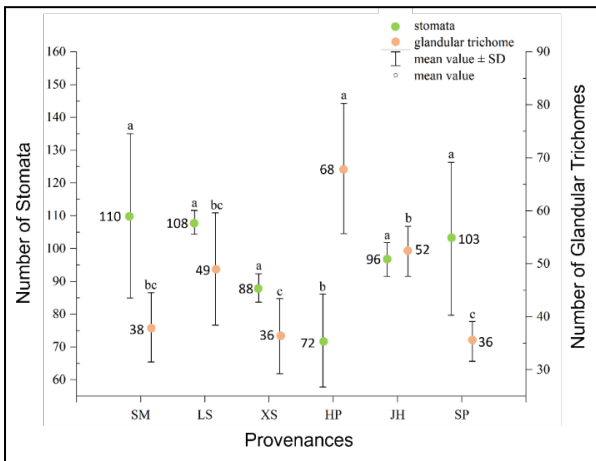


**Figure 11.** Box plots showing the number of stomata and glandular trichomes in six *Cyclocarya paliurus* provenances. The circles represent mean values, and the upper and lower whiskers represent  $\pm$  standard deviation. Different lowercase letters indicate significant differences ( $p \leq 0.05$ , LSD test). XS: Xiushui; SM: Shimen; LS: Lushan; JH: Jianghua; HP: Hupingshan; SP: Shuangpai.

### 3.7. Productivity Levels of Leaves from *C. paliurus* Provenances

Analysis of leaf productivity across six *C. paliurus* provenances revealed significant variation in photosynthetic efficiency and yield potential. Quantitative assessment of high-yield traits of six provenances using a productivity index (N) revealed the values (Eq. 7) ranged from 1664.72 to 2506.97 (Table 4), ranking as SM > SP > XS > JH > HP > LS. SM achieved the highest productivity, 50.6% greater than that of LS, indicating superior photosynthetic efficiency and yield potential. These findings identify SM as a promising germplasm resource for tea garden-style cultivation of *C. paliurus*.

The observed differences in productivity among the six *C. paliurus* provenances appear to be associated with environmental heterogeneity across their native habitats. Provenances originating from regions with moderate thermal ranges and mid-elevation conditions (e.g., SM and SP) exhibited the highest productivity under common-garden cultivation, suggesting that long-term exposure to relatively stable temperature regimes may have favored the evolution of higher photosynthetic capacity. In contrast, provenances such as LS and XS, which experience the coldest historical minimum temperatures and the widest thermal fluctuations, showed comparatively lower productivity, consistent with the expectation that colder environments promote more conservative carbon-gain strategies. Similarly, the mid- to low performance of high-altitude provenance HP may reflect adaptation to cooler, high-elevation conditions that limit photosynthetic investment. Although all provenances were cultivated under identical plantation conditions, the overall pattern indicates that productivity potential is at least partly shaped by provenance-specific environmental conditions, particularly temperature extremes and altitude gradients.

Although all provenances were grown in the same plantation site, the patterns suggest that historical environmental pressures—particularly temperature extremes and altitude—likely influenced the development of photosynthetic traits that determine productivity in the plantation site.

### 3.8. Principal Component Analysis of Leaf Traits of *C. paliurus* Provenances

Principal component analysis (PCA) applied for leaf structural traits of *C. paliurus* to identify key sources of phenotypic variance extracted four components, explaining 98.49% of total variance (Table 5). The four components explained 98.49% of the total variation, providing a robust basis for comprehensive evaluation. The first component (53.43%) was driven mainly by leaf width, chlorophyll content, and perimeter, reflecting core morphological and physiological functions linked to growth and photosynthetic potential. The second component (24.21%) emphasized anatomical traits, especially palisade thickness, P/LT and S/LT ratios, and productivity index, highlighting structural features critical for photosynthetic efficiency and stress tolerance. The third component (14.98%) related to water-holding capacity and morphological ratios, while the fourth (5.88%) correlated with productivity index, reflecting resource allocation. Cluster analysis based on 27 structural traits grouped the six provenances into three subgroups (Figure 12). The dendrogram was constructed using hierarchical clustering with Euclidean distance and the unweighted pair-group method. The y-axis indicates the provenances, and the x-axis represents the linkage distance, where shorter distances reflect higher similarity in leaf characteristics, whereas longer distances indicate greater divergence among provenances. HP, LS, SP, and SM formed subgroup I, characterized by similar palisade development and high P/S ratios, though SM showed partial divergence. JH formed subgroup II, distinguished by greater palisade and leaf thickness. XS stood alone in subgroup III, representing the most divergent anatomical profile with relatively weak palisade development, consistent with PCA results.

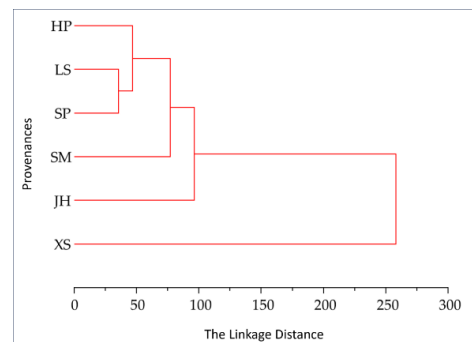


**Figure 12.** Cluster analysis of *Cyclocarya paliurus* provenances based on morphological, anatomical, and physiological leaf traits. XS: Xiushui; SM: Shimen; LS: Lushan; JH: Jianghua; HP: Hupingshan; SP: Shuangpai

**Table 5.** Principal component analysis (PCA) of morphological, anatomical, and physiological traits of *Cyclocarya paliurus* leaves

	Component			
	1	2	3	4
Leaf Area	0.889	-0.401	-0.036	0.213
Perimeter	0.949	-0.236	-0.205	0.034
Vertical Length	0.821	-0.523	-0.031	0.219
Horizontal Width	0.961	-0.135	-0.231	0.052
Aspect Ratio	0.202	0.793	-0.351	-0.353
Leaf Shape Coefficient	-0.318	-0.539	0.572	0.528
LT	0.309	-0.380	0.705	-0.507
SPAD	0.960	0.133	0.083	-0.012
Fresh Leaf Weight	0.916	-0.300	0.175	0.203
Saturated Fresh Leaf Weight	0.927	-0.294	0.117	0.203
Dry Leaf Weight	0.862	-0.368	0.329	0.088
Relative Water Content of Leaf	-0.711	0.058	0.698	0.052
Specific Leaf Area	0.646	-0.218	-0.691	0.237
Leaf Tissue Density	-0.959	0.060	0.166	0.224
Leaf Dry Matter Fraction	-0.914	0.076	0.387	-0.084
TU	0.504	0.716	0.463	0.029
TP	-0.368	0.911	0.014	0.129
TS	0.600	0.726	0.329	-0.016
TL	0.671	0.597	0.380	-0.013
Stomatal Number on the Lower Epidermis	0.212	-0.061	-0.780	-0.480
Petiole Thickness	-0.911	-0.309	-0.254	0.074
P/S	-0.432	0.749	-0.414	0.282
P/L	-0.732	-0.665	-0.052	0.003
U/S	0.833	0.353	0.419	0.021
S/P	0.517	0.851	0.025	0.069
S/LT	0.894	-0.306	-0.308	-0.065
Y	-0.908	-0.311	-0.261	0.074
N	-0.099	0.670	-0.441	0.578
Eigenvalue	14.96	6.78	4.19	1.65
Variance Contribution Ratio	53.43	24.21	14.98	5.88
Cumulative Contribution Ratio	53.43	77.63	92.61	98.49

\* Variance contribution ratios, and cumulative contribution ratios of the first four principal components (PC1–PC4) are shown. **TU**: upper epidermis thickness; **TP**: palisade

tissue thickness; **TS**: spongy tissue thickness; **TL**: lower epidermis thickness; **P/S**: ratio of palisade tissue thickness to spongy tissue thickness; **P/L**: palisade tissue thickness to leaf thickness; **U/S**: upper epidermis thickness to spongy tissue thickness; **S/P**: spongy tissue thickness to palisade tissue thickness; **S/L**: spongy tissue thickness to leaf thickness; **N**: productivity index; **Y**: cold resistance score.

### 3.9. Stress Resistance Levels of Leaves from *C. paliurus* Provenances

#### 3.9.1. Pest and disease, drought, and cold resistance

Drought, disease and pest, cold, and stress resistance indices were calculated from corresponding anatomical and physiological parameters. A pest and disease resistance assessment using four leaf anatomical indicators, including palisade thickness, epidermal thickness, total leaf thickness, and the P/S ratio, and the membership function method (Eq. 10) revealed notable differences in disease and pest resistance levels, and a clear contrast in adaptive capacity among the six *C. paliurus* provenances. The results (Table 6) showed that the average membership function values of all samples ranged from 0.37 to 0.58, with a mean value of 0.45, exceeding the 0.35 threshold for strong resistance. SP showed the highest resistance value (0.58), indicating a markedly stronger ability to withstand pathogenic and pest pressures compared to all other provenances. LS and XS (0.46) also demonstrated relatively strong resistance, suggesting moderate inherent defense mechanisms. HP (0.42) and SM (0.40) exhibited only average levels of resistance, indicating a more limited but still functional defensive capacity. In contrast, JH had the lowest resistance score (0.37), making it the most susceptible source in terms of vulnerability to disease and pest damage. Overall, the results highlight SP as the most promising provenance for environments with high biotic stress, while JH may require additional management strategies to mitigate pest and disease risks.

**Table 6.** Comprehensive evaluation of resistance-related indices in *Cyclocarya paliurus* provenances

Seed Source	LT	TU	TP	TL	P/S	Drought Resistance	Disease and Pest Resistance	Cold Resistance	Stress Resistance
HP	0.41	0.50	0.45	0.42	0.39	0.42	0.42	2.57	1.14
JH	0.39	0.57	0.39	0.36	0.33	0.37	0.37	2.15	0.96
LS	0.48	0.50	0.50	0.53	0.41	0.48	0.46	3.83	1.59
SM	0.36	0.61	0.40	0.47	0.46	0.42	0.40	3.84	1.55
SP	0.60	0.63	0.56	0.41	0.56	0.53	0.58	2.82	1.31
XS	0.41	0.44	0.41	0.61	0.56	0.50	0.46	5.37	2.11
Average	0.44	0.54	0.45	0.47	0.45	0.45	0.45	3.43	1.44

\* Values represent provenance means; average values are shown at the bottom. **LT**: leaf thickness; **TU**: upper epidermis thickness; **TP**: palisade tissue thickness; **TL**: lower epidermis thickness; **P/S**: ratio of palisade tissue thickness to spongy tissue thickness. **XS**: Xiushui; **SM**: Shimen; **LS**: Lushan; **JH**: Jianghua; **HP**: Hupingshan; **SP**: Shuangpai.

Drought and cold resistance assessment using palisade thickness, leaf thickness, and the P/S ratio produced the drought and cold resistance membership function values (Eq. 8) of 0.37–0.58 and 2.15–5.37, with mean values of 0.45 and 3.43, respectively (Table 6). SP exhibited the strongest drought resistance (0.53), far exceeding all other provenances, while XS (0.50) and LS (0.48) also demonstrated high drought tolerance, forming a secondary resilient group. In contrast, SM (0.42) and HP (0.42) showed only moderate drought resistance, and JH (0.37) ranked lowest, indicating limited capacity to withstand water stress. Cold resistance followed a somewhat different pattern: XS (5.37) showed the greatest tolerance to low temperatures, suggesting superior adaptation to colder climates, whereas SM (3.84) and LS (3.83) displayed moderate cold resilience. SP (2.82) and HP (2.57) exhibited lower resistance than average. JH (2.15) had the weakest score for cold resistance.

Stress resistance assessment using palisade thickness, leaf thickness, and the P/S ratio produced the stress resistance membership function values of 0.96–02.11, with an average of 1.44 (Table 6). XS exhibited the strongest stress resistance (2.11), far exceeding all other provenances, while LS (1.59) and SM (1.55) also demonstrated high stress tolerance, forming a secondary resilient group. In contrast, SP (1.31) and HP (1.14) showed lower stress resistance than the average, and JH (0.96) ranked lowest, indicating limited capacity to withstand stress.

The integrated resistance assessment revealed clear provenance-level differences in adaptive capacity among *C. paliurus*. SP exhibited the strongest pest, disease, and drought resistance, while XS showed superior cold and overall stress tolerance. LS and SM formed a moderately resilient group across most indices, whereas HP displayed only average performance. JH consistently ranked lowest, indicating the weakest biotic and abiotic stress resistance.

The stress adaptations exhibited by the six natural populations (HP, JH, LS, SM, SP, XS) of *C. paliurus* in the same plantation site appear to be closely related to environmental factors such as extreme temperatures, humidity, precipitation, and altitude in the region where they originate. For temperature regimes and cold

adaptation, provenances originating from colder and more thermally variable regions, such as XS and LS, exhibit structural traits that enhance tolerance to low temperatures. XS, which experiences the lowest historical minimum temperatures (-11.6 °C) and wide thermal fluctuations, shows the thinnest epidermis and mesophyll layers, high glandular trichome density, and the highest cold resistance score (5.37). LS also exhibits moderate cold resilience. In contrast, JH and HP, which experience milder winter temperatures (-4.8 °C to -6.5 °C), display thicker leaf tissues and lower cold resistance, reflecting adaptation to less extreme climates. For drought adaptation, provenances such as SP, XS, and LS, originating from regions with high or variable precipitation, demonstrate high drought resistance (membership function values: SP: 0.53; XS: 0.50; LS: 0.48). These provenances combine efficient hydraulic structures with protective anatomical features (e.g., trichomes and cuticle development) to mitigate water stress. Conversely, JH, from a consistently humid environment, shows limited drought resistance (0.37), indicating lower selective pressure for water-conserving traits. For biotic stress adaptation, SP exhibits the strongest resistance to pests and diseases (0.58), consistent with its native habitat conditions that may impose higher biotic stress pressures. LS and XS show moderate biotic stress tolerance (0.46), while JH displays the weakest defense mechanisms (0.37), reflecting lower evolutionary pressure from pathogens and herbivores in humid, warm habitats.

#### 4. DISCUSSION

Plants have developed various strategies to adapt to different ecological environments, in which phenotypic plasticity serves as a key mechanism in response during the long-term evolutionary process. As the primary organ for photosynthesis, transpiration, and respiration, leaves are directly exposed to environmental factors, rendering them highly sensitive and thus strongly plastic (Chen et al., 2018; Zeng and Wang, 2019), which makes them an important indicator for evaluating plant adaptability and production potential. In studies of economically important plants such as tea trees, it has been reported that the anatomical structure of wild tea leaves is often used as a critical metric to assess physiological activity, stress resistance, yield, and



quality (Zhu and Huang, 2015). Therefore, systematic analysis of leaf structure can provide a valuable morphological basis for the targeted selection and breeding of *C. paliurus* for tea-style cultivation. This study provides a comprehensive evaluation of morphological, anatomical, and physiological traits of *C. paliurus* leaves across six provenances in China under tea plantation-style cultivation. Our findings are consistent with previous study on introduction and cultivation of representative geographical sources of *C. paliurus* from Xiushui (Jiangxi Province), Zhangjiajie (Hunan Province) and Shennongjia (Hubei Province) origins to the same plantation site located in Wuhan (Hubei Province) in order to select excellent provenances suitable for planting in the Wuhan region, and reported the rich variation of leaf traits and diverse photosynthetic characteristics among the provenances (Qiu, 2024). Such diversity provides valuable opportunities for germplasm selection but also presents challenges for standardizing large-scale cultivation.

As shown in Table 1, the six provenances of *C. paliurus* originate from ecologically diverse regions characterized by substantial variation in historical temperature extremes, mean annual temperature, humidity, precipitation, and especially altitude. Provenances such as XS and LS are native to environments with colder historical minima, while JH and HP experience milder winters. For altitudinal differences, HP originates from high elevations, and most other provenances from mid-elevational habitats. In contrast, the plantation site is located at a much lower elevation, representing a notably warmer and less variable thermal environment relative to the native habitats. Provenances originating from environments more similar in temperature, precipitation, humidity, and altitude to the plantation conditions tend to exhibit stronger early growth. This highlights the importance of considering provenance-specific ecological adaptation when selecting germplasm for large-scale cultivation and supports the use of environmental-matching strategies to optimize plantation performance and leaf yield. This climatic and ecological heterogeneity likely shapes local adaptation patterns across provenances and provides an important context for understanding differences in growth performance under uniform cultivation conditions.

Seedling growth traits differed significantly among the six provenances (Table 2). LS exhibited the strongest early growth, with the greatest seedling height and basal stem diameter. SM ranked second and showed growth metrics statistically comparable to LS, underscoring their superior vigor under plantation conditions. In contrast, JH displayed the poorest performance for both traits, suggesting lower adaptability or reduced plasticity in the plantation environment. The remaining provenances (HP, SP, and XS) showed intermediate levels of growth.

Significant morphological and anatomical variation among *C. paliurus* provenances indicates clear provenance-specific adaptations to differing environmental conditions. Although HP provenance exhibited the largest leaf area, it

had a relatively low productivity index. In contrast, SM provenance, with the second largest leaf area, showed the highest productivity index. This may be due to a relative decrease in leaf thickness as leaf area increases (Guo and Wu, 2018), which in turn reduces the thickness of the palisade tissue. Since palisade tissue thickness is strongly positively correlated with photosynthetic intensity (Zhu and Huang, 2015), the expansion of leaf area, although beneficial for increasing light interception (Wang et al., 2024), tends to result in a sparse distribution of palisade tissue. Given that chlorophyll is primarily distributed within the palisade tissue, its content determines the efficiency of light energy capture and carbon assimilation. Furthermore, the report on tea plants indicated that cell density and palisade tissue thickness are highly correlated with leaf productivity (Dong et al., 2024). Within a measurement range of  $N=400 \mu\text{m}$ , SM provenance exhibited the highest number of first-layer palisade cells, suggesting the densest cell arrangement. The synergistic effect of a large leaf area and compact palisade tissue contributed to its highest productivity, making it an ideal germplasm resource for tea garden-oriented selection.

Organic matter accumulation closely followed photosynthetic activity, confirming the theoretical foundation proposed (Liu et al., 2016), stating that differences in leaf anatomical structure might be correlated with yield. The observed differences in productivity among the six *C. paliurus* provenances appear to be associated with environmental heterogeneity across their native habitats. Provenances originating from regions with moderate thermal ranges and mid-elevation conditions (SM and SP) exhibited the highest productivity under common-garden cultivation, suggesting that long-term exposure to relatively stable temperature regimes may have favoured the evolution of higher photosynthetic capacity. In contrast, provenances such as LS and XS, which experience the coldest historical minimum temperatures and the widest thermal fluctuations, showed comparatively lower productivity, consistent with the expectation that colder environments promote more conservative carbon-gain strategies. Similarly, the mid- to low performance of high-altitude provenance HP may reflect adaptation to cooler, high-elevation conditions that limit photosynthetic investment. Although all provenances were cultivated under identical plantation conditions, the overall pattern indicates that productivity potential is at least partly shaped by provenance-specific environmental conditions, particularly temperature extremes and altitude gradients.

Leaf thickness, chlorophyll content, and specific leaf area (SLA) also align with provenance-specific climatic adaptation. LS, which produced the thickest leaves, derives from habitats with cold winters, where increased leaf thickness supports greater mesophyll development and enhances photosynthetic capacity under low temperatures. JH, despite exhibiting weaker seedling growth overall, recorded the highest chlorophyll content, likely reflecting adaptation to high humidity and warm

temperatures that favour increased chlorophyll investment for efficient light capture in shaded or diffuse-light environments. Meanwhile, SM demonstrated the highest SLA, a characteristic associated with high-light environments and fast growth strategies, consistent with its mid-elevation origin and more favourable climatic conditions. Taken together, the clear biomass differentiation among provenances under uniform plantation conditions underscores the strong influence of native environmental factors—such as temperature extremes, humidity regimes, precipitation, and altitude—on leaf structural and physiological traits. These inherent differences reflect long-term climatic adaptation and significantly shape the biomass potential of each provenance. Understanding these linkages is essential for selecting high-performing germplasm for tea-style plantation cultivation and for optimizing leaf yield in future industrial applications.

The anatomical differences among *C. paliurus* provenances are closely linked to the environmental and climatic conditions of their native habitats. Provenances from warm, humid regions (JH) develop thicker epidermal layers and more extensive mesophyll tissues to enhance photosynthesis and gas exchange. In contrast, provenances from colder or more stressful climates (XS) show thinner tissues and more protective features, reflecting conservative strategies suited to low temperatures and environmental stress. Variation in stomatal density, trichome density, and petiole thickness also mirrors the climatic origins of each provenance—those from high-light or humid environments exhibit higher stomatal density and stronger vascular capacity, while those from colder or variable climates invest more in protective structures like trichomes and dense cuticles. Overall, these anatomical traits represent long-term adaptations to each provenance's native climate and persist even when plants are grown under the same plantation conditions. Our findings are strongly correlated with previous studies reporting that environmental factors such as temperature extremes, humidity regimes, precipitation, and altitude affect the leaf structural and physiological traits of *C. paliurus* provenances, suggesting that these factors contribute to the environmental heterogeneity across their native habitats, influencing their adaptability and growth (Sun et al., 2021; Feng et al., 2022).

In addition, recent studies have revealed that terpenoids and polysaccharides in *C. paliurus* are mainly synthesized in the palisade tissue, whereas flavonoids are predominantly distributed in glandular hairs and epidermal tissues (Zhou et al., 2017). Jianghua provenance, possessing the greatest thickness of palisade and spongy tissue as well as a relatively high density of glandular trichome, may hold significant advantages in the biosynthesis and accumulation of functional bioactive compounds, offering valuable germplasm for the development of high value-added products. Meanwhile, research into whether there is a correlation between the

metabolite content and leaf anatomical structure of JH-origin plants, which are thought to be particularly rich in terpenoids, will form a basis for functional product development and molecular breeding.

Stress resistance evaluation using the membership function method indicated that *C. paliurus* generally exhibits high resistance to environmental stresses, but with notable inter-provenance variation. SP provenance showed outstanding drought and pest resistance (scores of 0.53 and 0.58, respectively). XS provenance, characterized by compact cellular structure and a high P/S tissue ratio, demonstrated the strongest cold resistance (score of 5.37), and thus exhibits superior environmental adaptability. These findings are consistent with the previous report on leaf anatomy and physiological characteristics of tea trees in Ailaoshan Qianjiazhai National Nature Reserve (Yunnan, China) (Hou et al., 2023), which suggested that provenances with higher P/S ratios, well-developed cell wall structures, and tightly arranged cells generally possess better environmental adaptability. Because all grafted seedlings were cultivated under uniform plantation conditions without exposure to actual biotic or abiotic stresses, the resistance indices generated in this study represent indirect assessments derived solely from calculated leaf traits, measured parameters, and associated formulas rather than from direct stress responses. However, in parallel with our findings, previous findings have shown that *C. paliurus* provenances exhibit varied responses to direct stress conditions, including salinity, cold, and shading, and can enhance their growth and physiological performance under stress conditions, as well (Deng et al., 2017; Zhang et al., 2023; Zhang et al., 2025)

Cluster analysis divided the six provenances into three distinct groups: Hupingshan, Lushan, Shuangpai, and Shimen formed the first group, characterized by high photosynthetic efficiency and strong stress resistance; Jianghua alone constituted the second group, with balanced anatomical traits; Xiushui, due to its unique cold tolerance and efficient resource utilization traits, was classified into the third group. In conclusion, Shimen and Shuangpai provenances, with their high photosynthetic efficiency and robust stress resistance, are promising candidates as high-quality germplasm for tea garden cultivation. Xiushui provenance, with desirable traits related to cold resistance and resource-use efficiency, could be promoted in cold or arid regions following targeted breeding of relevant traits.

The observed anatomical and physiological differentiation among *C. paliurus* provenances underscores the influence of environmental and climatic factors on stress adaptation. Provenances from cold, variable, or stress-prone habitats prioritize structural and protective traits for survival, while those from warm, humid environments invest in growth-optimized traits, reflecting a functional trade-off between stress tolerance and photosynthetic capacity. These findings provide a theoretical basis for provenance



selection in leaf-based industrial cultivation under tea-style plantation systems. When combined across biotic and abiotic stress indices, XS demonstrates the highest overall stress tolerance (2.11), SP excels in drought and biotic stress adaptation (1.31), LS and SM form a moderately resilient group (1.59 and 1.55), HP shows average resistance (1.14), and JH consistently ranks lowest (0.96). These patterns reinforce the strong linkage between provenance-specific anatomical traits and their native environmental conditions.

These results not only strengthen the theoretical basis for using anatomical traits as predictors of agronomic performance but also provide practical criteria for early germplasm screening in breeding programs. Importantly, the diversity in functional adaptations among provenances indicates that no single population possesses a complete suite of desirable traits, reinforcing the need for integrative breeding strategies combining high yield, stress resilience, and quality traits. Nevertheless, limitations exist. This study was conducted under a single ecological site, and genotype–environment interactions may further modulate leaf traits and metabolite accumulation. Long-term trials across different ecological zones, combined with molecular marker-assisted selection, are needed to validate and refine these findings. Overall, the results underscore the potential of targeted provenance selection to advance *C. paliurus* cultivation. By integrating leaf structural evaluations with functional trait analyses, this study provides both theoretical insight and practical guidance for the industrial development of this emerging multipurpose species.

#### 4. CONCLUSION

This study demonstrated substantial inter-provenance variation in the morphological, anatomical, and physiological traits of *Cyclocarya paliurus* under tea plantation-style cultivation. Shimen provenance exhibited the highest productivity potential, Jianghua showed enhanced stress adaptability through superior chlorophyll content and epidermal traits, Hupingshan displayed adaptive mechanisms via large leaves and dense trichomes, and Xiushui demonstrated exceptional cold resistance despite low biomass accumulation. Collectively, these findings highlight the diverse adaptive strategies of different provenances and the rich genetic resources available for targeted breeding. Key structural indicators, particularly palisade-to-spongy tissue ratio, leaf thickness, and epidermal development, emerged as reliable predictors of productivity and stress resistance. Also, differences in geographic origin can reflect distinct ecological and genetic backgrounds, which may contribute to the observed variations in morphological, anatomical, and physiological traits among provenances growing in the

same plantation site. These results not only reinforce the utility of anatomical analyses for germplasm evaluation but also provide a scientific basis for the directional selection of elite cultivars. Future efforts should expand to multi-environment trials and integrate molecular approaches to validate genotype–environment interactions and accelerate breeding. Overall, this work provides theoretical support and empirical evidence to guide the sustainable cultivation and industrial development of *C. paliurus* in tea plantation systems.

#### Acknowledgment

We are grateful to the Hunan Provincial Forestry Science and Technology Innovation and Development Office in China for providing a financial support (Project Grant # XLKY202311) to conduct this research.

#### Author Contribution

Rui CHEN: (a) Original Idea, (b) Study Design, Methodology, (c) Literature Review, (f) Data Collection, (g) Data Analysis, (h) Drafting Article, (i) Critical Review

Seyit YUZUAK: (b) Study Design, Methodology, (c) Literature Review, (d) Supervision, (g) Data Analysis, Interpretation, (h) Drafting Article, (i) Critical Review

Min WU: (f) Data Collection, (e) Material, Resource Supply

Fangping TONG: (f) Data Collection, (e) Material, Resource Supply

Sen LIU: (d) Supervision, (e) Material, Resource Supply

Gui LI: (a) Original Idea, (b) Study Design, Methodology, (d) Supervision, (e) Material, Resource Supply, (f) Data Collection, (g) Data Analysis, Interpretation, (h) Drafting Article, (i) Critical Review

#### Ethical Statement

In this study, we affirm that all the necessary rules under the "Regulation on Scientific Research and Publication Ethics in Higher Education Institutions" have been adhered to, and none of the actions mentioned under the title "Actions Contrary to Scientific Research and Publication Ethics" in the mentioned regulation have been conducted.

#### Conflict of Interest

The authors report there are no competing interests to declare.

#### REFERENCES

Chen, X. F., Jing, C. J., Zhao, X. P., & Wu, X. H. (2018). Advances in the application of plant leaf tissue structure in the research of stress tolerance. *Journal of Hebei Agricultural Sciences*, 22(3),

50–53. <https://doi.org/10.16318/j.cnki.hbnykx.2018.03.012>

Deng, B., Fang, S., Shang, X., Fu, X., & Li, Y. (2017). Influence of provenance and shade on biomass production and

- triterpenoid accumulation in *Cyclocarya paliurus*. *Agroforestry Systems*, 93, 483–492. <https://doi.org/10.1007/s10457-017-0138-x>
- Dong, F., Tu, J., Yang, F. Y., Dong, Y., Wu, Y. K., Chen, Q. C., Jin, L. L., & Xie, F. (2024). Comprehensive evaluation of 17 tea germplasm resources in Jiangxi based on leaf anatomical structure characteristics. *Acta Agriculturae Universitatis Jiangxiensis*, 46(2), 328–339. <https://doi.org/10.3724/aaui.2024030>
- Fang, S. Z., Wang, J. Y., Wei, Z. Y., & Zhu, Z. X. (2006). Methods to break seed dormancy in *Cyclocarya paliurus* (Batal) Iljinskaja. *Scientia Horticulturae*, 110(3), 305–309. <https://doi.org/10.1016/j.scienta.2006.06.031>
- Fang, S. Z., & Wang, J. Y. (2007). Changes in biochemical composition and enzyme activity during dormancy release of *Cyclocarya paliurus* seeds. *Forestry Studies in China*, 9, 7–13. <https://doi.org/10.1007/s11632-007-0002-6>
- Feng, Y., Zheng, K., Lin, X., & Huang, J. (2022). Plant growth, physiological variation and homological relationship of *Cyclocarya* species in ex situ conservation. *Conservation Physiology*, 10(1). <https://doi.org/10.1093/conphys/coac016>
- Guo, C. L., Liu, S. X., Xiao, R. C., Su, X. N., Liu, W. H., Hu, X. F., & Jiang, R. X. (2024). Research progress on breeding technology of *Cyclocarya paliurus*, a rare plant of single species in China. *Chinese Wild Plant Resources*, 43(8), 64–69. <https://doi.org/10.3969/j.issn.1006-9690.2024.08.010>
- Guo, S. J., & Wu, Y. Q. (2018). Leaf anatomical structure characteristics and drought resistance of Chinese chestnut. *Journal of Northwest A&F University (Natural Science Edition)*, 46(9), 51–59. <https://doi.org/10.13207/j.cnki.jnwafu.2018.09.007>
- Guo, W. W., Zuo, M. C., Han, J. H., & Fang, J. P. (2024). Anatomical structure and stress resistance evaluation of leaves of *Rhododendron* L. in Shergyla Mountain. *Journal of Henan Agricultural Sciences*, 53(6), 111–119. <https://doi.org/10.15933/j.cnki.1004-3268.2024.06.012>
- Hou, M. Y., Wang, F., Chen, M., Cheng, X. M., Luo, W., & Huang, X. X. (2023). Leaf anatomical structure and physiological characteristics of wild and cultivated tea trees in Qianjiashai. *Chinese Journal of Ecology*, 42(5), 1074–1082. <https://doi.org/10.13292/j.1000-4890.202305.011>
- Lan, L. X., Xu, Z. H., Sun, C. W., & Fang, S. Z. (2022). Evaluation of germplasm resources for *Cyclocarya paliurus* and screening of superior families and individual trees. *Forest Research*, 35(5), 42–51. <https://doi.org/10.13275/j.cnki.lykxyj.2022.005.005>
- Li, C. H. (2024). *Physiological and molecular mechanisms of Cyclocarya paliurus in response to drought stress* [Doctoral dissertation, Nanjing Forestry University]. <https://doi.org/10.27242/d.cnki.gnjlu.2024.000002>
- Liu, R., Cao, Y. H., Zhang, C. H., Zhang, X. W., Du, W. B., Wang, X. H., Zhang, Y. Q., Wang, R. L., & Zhou, X. L. (2025). Effects of functional traits of *Zanthoxylum bungeanum* 'Dahongpao' leaves of different ages on yield in Wudu District, Longnan City. *Non-wood Forest Research*, 43(2), 166–174. <https://doi.org/10.14067/j.cnki.1003-8981.2025.02.018>
- Liu, X. L., Song, Z. Q., Hu, F. R., & Sang, X. L. (2024). A comparative study on leaf characters between diploid and tetraploid *Cyclocarya paliurus*. *Journal of Nanjing Forestry University (Natural Science Edition)*, 48(4), 76–84. <https://doi.org/10.12302/j.issn.1000-2006.202305024>
- Liu, Y., Qian, C., Ding, S., Shang, X., Yang, W., & Fang, S. (2016). Effect of light regime and provenance on leaf characteristics, growth and flavonoid accumulation in *Cyclocarya paliurus* (Batal) Iljinskaja coppices. *Botanical Studies*, 57, 28. <https://doi.org/10.1186/s40529-016-0145-7>
- Liu, Y., Cao, Y. N., Fang, S. Z., Wang, T. L., Yin, Z. Q., Shang, X. L., Yang, W. X., & Fu, X. X. (2018). Antidiabetic effect of *Cyclocarya paliurus* leaves depends on the contents of antihyperglycemic flavonoids and antihyperlipidemic triterpenoids. *Molecules*, 23(5), 1042. <https://doi.org/10.3390/molecules23051042>
- Liu, Y., Luo, W. M., Duan, R. Y., Li, Y., & Yang, X. Z. (2022). Study on drought-resistant tea cultivars in Weining County. *Southwest China Journal of Agricultural Sciences*, 35(3), 530–535. <https://doi.org/10.16213/j.cnki.scjas.2022.3.007>
- Liu, Y. L., Ye, L. J., Kou, Y. X., Fan, D. M., Zhang, Z. Y., & Cheng, S. M. (2022). Population genetic structure and gene flow in natural populations of *Cyclocarya paliurus* in Jiangxi Province. *Acta Agriculturae Universitatis Jiangxiensis*, 44(4), 938–947. <https://doi.org/10.13836/j.jjau.2022093>
- Qing, X., Zhu, J. J., Guan, X. Y., Yu, X. Y., & Cao, K. F. (2017). Association of leaf anatomical structure characteristics with photosynthetic capacity and drought tolerance in seven sugarcane varieties. *Plant Physiology Journal*, 53(4), 705–712. <https://doi.org/10.13592/j.cnki.ppj.2017.0038>
- Qiu, M. X. (2024). *Adaptability analysis of Cyclocarya paliurus provenance and research on flavonoid gene mining and breeding of excellent provenance* [Master's thesis, South China Agricultural University]. <https://doi.org/10.27158/d.cnki.ghznu.2024.001907>
- Sang, X. L., Li, Q. Q., Deng, B., & Fang, S. Z. (2014). Effects of light intensity and fertilization on leaf traits and anatomical structure of *Cyclocarya paliurus*. *Journal of Southwest Forestry University*, 34(6), 9–15. <https://doi.org/CNKI:SUN:YNLX.0.2014-06-002>
- Sun, C., Zhou, Y., Fang, S., & Shang, X. (2021). Ecological Gradient Analysis and Environmental Interpretation of *Cyclocarya paliurus* Communities. *Forests*, 12(2), 146. <https://doi.org/10.3390/f12020146>
- Sun, C. W., Shang, X. L., Fang, S. Z., Yang, W. X., Cao, Y. N., Ding, H. F., & Li, C. X. (2022). Association analysis between genotype and environment: Differentiation between *Cyclocarya paliurus* resources that accumulate triterpenoids. *Frontiers in Plant Science*, 13, 945897. <https://doi.org/10.3389/fpls.2022.945897>
- Wang, F. Q., Li, J. Y., Feng, H., Luo, S. C., Lin, M. J., Li, S. H., Zhang, J. M., Zhang, B., & Chen, R. B. (2019). Analysis of leaf anatomical structure of Wuyi Mingcong tea germplasm resources. *Chinese Journal of Tropical Crops*, 40(12), 2375–2389. <https://doi.org/10.3969/j.issn.1000-2561.2019.12.010>
- Wang, J., Li, P., Li, N., Lan, L. X., Shang, X. L., & Fang, S. Z. (2023). Variations in growth, leaf anatomical structure, and photosynthetic pigment content of *Cyclocarya paliurus* clones. *Journal of West China Forestry Science*, 52(2), 132–137. <https://doi.org/10.16473/j.cnki.xblykx1972.2023.02.018>
- Wang, S. Y., Tian, L., Zhou, S. T., Chu, Y. E., Mei, D., Yuan, J. Q., Yu, Y. H., & Fu, X. X. (2024). Effects of polyploidization on leaf morphology, photosynthetic performance, and accumulation of secondary metabolites in *Cyclocarya paliurus*. *Scientia Silvae Sinicae*, 60(8), 120–131. <https://doi.org/10.11707/j.1001-7488.lykx20230322>
- Wang, Y. B., Liu, W., Li, W., Wang, C. J., Dai, H. Y., Xu, R., Zhang, Y. E., & Zhang, L. F. (2024). Effect of light intensity on leaf photosynthetic physiology and root system of sweet potato in the early stage of growth. *Acta Agronomica Sinica*, 50(10), 2575–2585. <https://doi.org/10.3724/SP.J.1006.2024.44011>
- Xu, R. C., Zhang, P., & Xiang, M. (2023). Research progress on chemical constituents and anti-metabolic disease pharmacological effects of *Cyclocarya paliurus*. *Chinese Traditional and Herbal Drugs*, 54(9), 2962–2977. <https://doi.org/10.7501/j.issn.0253-2670.2023.09.029>



- Yang, C., Su, S. F., Yang, D. X., Liang, S. H., Guo, Y., Guo, C., & Chen, Z. W. (2024). Comparison of leaf anatomical structure and stress resistance of wild tea plants in Panzhou City and Sandu County, Guizhou Province. *Journal of Henan Agricultural Sciences*, 53, 48–61. <https://doi.org/10.15933/j.cnki.1004-3268.2024.01.006>
- Zeng, W. J., & Wang, D. X. (2019). Comprehensive evaluation of drought resistance based on leaf anatomical structure of *Camellia oleifera* 'Cenruan' series superior clones. *Southwest China Journal of Agricultural Sciences*, 32(11), 2492–2501. <https://doi.org/10.16213/j.cnki.scjas.2019.11.003>
- Zhao, W. J., Tang, D. B., Yuan, E., Wang, M., Zhang, Q. F., Liu, Y., Shen, B. Y., Chen, J. G., & Yin, Z. P. (2020). Induction and cultivation of novel red *Cyclocarya paliurus* callus and its unique morphological and metabolic characteristics. *Industrial Crops and Products*, 147, 112266. <https://doi.org/10.1016/j.indcrop.2020.112266>
- Zhang, Z., Gu, Y., Mao, Q., & Wang, J. (2023). Physiological Response to Low Temperature of Four Genotypes of *Cyclocarya paliurus* and Their Preliminary Evaluation to Cold Resistance. *Forests*, 14(8), 1680. <https://doi.org/10.3390/f14081680>
- Zhang, Z., Jin, H., Hong, K., & Fang, S. (2025). Effects of salicylic acid and brassinolide applications on salt tolerance in *Cyclocarya paliurus*: Amelioration of oxidative stress. *Tree Physiology*, 45(6). <https://doi.org/10.1093/treephys/tpaf061>
- Zhou, M. M., Qian, C. Y., Liu, Y., Fang, S. Z., Yang, W. X., & Shang, X. L. (2017). Observation on leaf anatomical structure and histochemical localization of flavonoids, triterpenoids, and polysaccharides in leaves of *Cyclocarya paliurus*. *Journal of Plant Resources and Environment*, 26(2), 107–109. <https://doi.org/10.3969/j.issn.1674-7895.2017.02.14>
- Zhu, Y., & Huang, Y. H. (2015). Research on the relationship between anatomical structure characteristics and traits of wild tea leaves in Jinxiu County, Guangxi. *Chinese Wild Plant Resources*, 34(4), 16–21. <https://doi.org/10.3969/j.issn.1006-9690.2015.04.004>